International Journal of Science and Research (IJSR)
ISSN: 2319-7064
Impact Factor 2025: 7.089

Erdheim-Chester Disease: A Rare Non-Langerhans Cell Histiocytosis with Pathognomonic Multisystem Imaging Findings: Case Report Illustrating the Classic Radiological Triad

Sachin Jain

Abstract: ***Background**: Erdheim–Chester disease (ECD) is a rare non-Langerhans cell histiocytic neoplasm characterised by xanthogranulomatous infiltration of multiple organ systems by foamy CD68-positive, CD1a-negative histiocytes. The condition produces a highly characteristic constellation of skeletal, retroperitoneal and cardiovascular imaging findings, and in the majority of cases the radiologist is the first physician to raise the diagnosis. **Case Presentation**: We report a case of ECD in a middle-aged male who presented with insidious bilateral knee pain, polyuria and incidentally detected renal impairment. Plain radiographs of both lower limbs demonstrated bilateral, symmetric metadiaphyseal osteosclerosis of the distal femora and proximal tibiae with characteristic sparing of the epiphyses. Contrast-enhanced computed tomography (CECT) of the abdomen revealed symmetric perinephric soft-tissue infiltration producing the "hairy kidney" appearance with thickened bridging perirenal septa, bilateral hydroureteronephrosis, and circumferential periaortic soft tissue extending from the descending thoracic aorta to the iliac bifurcation, constituting the "coated aorta" sign. CT of the thorax showed smooth interlobular septal thickening, pericardial thickening and a right atrial pseudotumour. Magnetic resonance imaging of the sella demonstrated loss of the posterior pituitary bright spot with infundibular thickening. Technetium-99m methylene diphosphonate (99mTc-MDP) bone scintigraphy showed intense symmetric tracer uptake in the distal femora and proximal tibiae. **Management and Outcome**: Image-guided biopsy of the perinephric soft tissue demonstrated foamy histiocytes within a fibrotic stroma that were immunoreactive for CD68 and negative for CD1a and S100, confirming the diagnosis. Molecular analysis identified a BRAF V600E mutation, and targeted therapy with a BRAF inhibitor was initiated. Interval imaging at six months showed regression of the periaortic and perinephric soft tissue with improvement in hydronephrosis. **Conclusion**: This case underscores the pivotal role of imaging in the recognition of ECD. The triad of bilateral symmetric metadiaphyseal osteosclerosis of the long bones, hairy kidneys and coated aorta is sufficiently distinctive to permit a confident radiological suggestion of the diagnosis, allowing targeted biopsy, molecular characterisation and early institution of MAPK-directed therapy.*

Keywords: Erdheim-Chester Disease, Histiocytosis Non-Langerhans-Cell, Tomography X-Ray Computed, Osteosclerosis, Retroperitoneal Fibrosis, Proto-Oncogene Proteins B-raf.

1. Introduction

Erdheim–Chester disease (ECD) is a rare multisystem non-Langerhans cell histiocytosis characterised by the infiltration of tissues by lipid-laden, foamy histiocytes surrounded by a dense fibrotic reaction. The condition was first described by the Austrian pathologist Jakob Erdheim and his American colleague William Chester in 1930 under the designation "lipoid granulomatosis". Fewer than 1,500 cases have been documented in the world literature, although increasing physician awareness and the widespread availability of cross-sectional imaging have driven a marked rise in diagnoses.

The nosological understanding of ECD was fundamentally revised in 2012, when activating BRAF V600E mutations were demonstrated in more than half of tested patients, establishing the disease as a clonal myeloid neoplasm rather than a reactive process. Subsequent work has identified additional activating mutations along the mitogen-activated protein kinase (RAS–RAF–MEK–ERK) pathway in the majority of BRAF wild-type cases. This reclassification carried immediate therapeutic consequences, providing the rationale for the use of BRAF and MEK inhibitors.

ECD predominantly affects adults in the fifth to seventh decades of life and demonstrates a distinct male preponderance. The clinical presentation is protean. Bone pain, most often affecting the knees and ankles, is the single most common symptom; other manifestations include central diabetes insipidus, exophthalmos, xanthelasma, retroperitoneal fibrosis with renal impairment, constitutional symptoms and neurological deficits.

From a radiological perspective, ECD is unusual among rare diseases in possessing a set of findings that are sufficiently characteristic to be considered virtually diagnostic when encountered in combination. Bilateral and symmetric osteosclerosis of the metaphyses and diaphyses of the long bones of the lower limbs, with sparing of the epiphyses and the axial skeleton, is regarded as the radiological hallmark. Within the abdomen, symmetric infiltration of the perinephric fat produces the "hairy kidney" appearance, while circumferential soft tissue encasing the aorta produces the "coated aorta" sign. Cardiac involvement, most characteristically an infiltrative right atrial pseudotumour, is frequently clinically silent yet carries prognostic significance.

Because histopathological examination in ECD is often non-specific, the diagnosis rests upon the integration of compatible histology with a characteristic clinical and radiological picture. Consequently, the radiologist occupies a central position in the diagnostic pathway.

2. Case Report

A middle-aged male patient presented to the outpatient department with a two-year history of insidious, symmetrical, deep aching pain around both knees and ankles, which was worse at night and had shown no response to non-steroidal anti-inflammatory therapy. He additionally reported polyuria and polydipsia of approximately one year's duration. There was no history of fever, weight loss, trauma, or prior malignancy. On examination the patient was afebrile and haemodynamically stable, with mild bilateral periorbital fullness and diffuse tenderness over the distal femora and proximal tibiae. Routine biochemistry revealed a raised serum creatinine with a normal serum calcium, phosphate and alkaline phosphatase, and elevated inflammatory markers.

Plain radiographs of both lower limbs were obtained as the initial investigation. These demonstrated striking bilateral and symmetric osteosclerosis involving the metaphyses and diaphyses of the distal femora, and the proximal and distal tibiae and fibulae. The sclerosis was patchy and coarse, with loss of the normal corticomedullary differentiation and mild cortical thickening. Characteristically, the epiphyses were entirely spared, and no periosteal reaction, cortical destruction or soft-tissue mass was identified. The axial skeleton appeared normal.

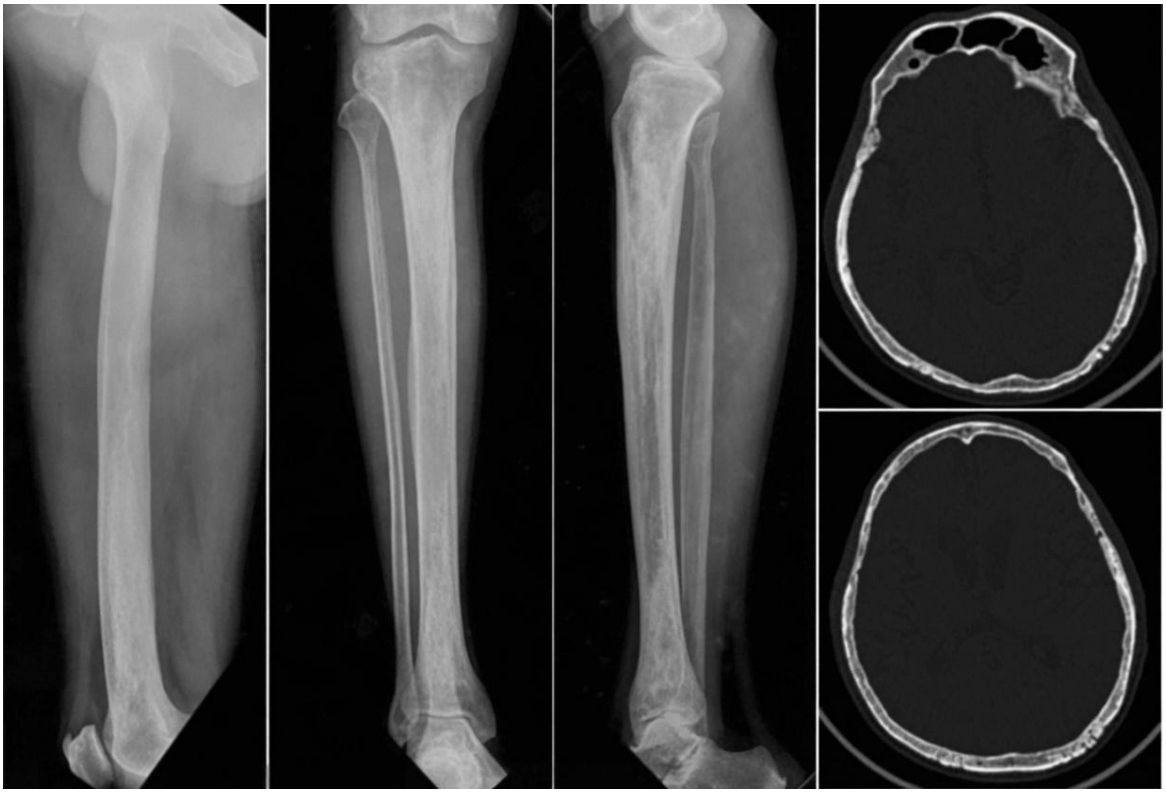

Figure 1: Anteroposterior radiographs of the lower limbs demonstrating bilateral, symmetric coarse osteosclerosis of the distal femoral and proximal tibial metadiaphyses with loss of corticomedullary differentiation and characteristic sparing of the epiphyses- the radiological hallmark of Erdheim–Chester disease

In view of the renal impairment, a contrast-enhanced computed tomographic (CECT) examination of the abdomen and pelvis was performed. This demonstrated bilateral, symmetric, ill-defined soft-tissue density infiltration of the perinephric fat, encasing both kidneys in a rind of tissue measuring approximately 20 to 30 Hounsfield units on the unenhanced series and showing only mild enhancement following intravenous contrast administration. The infiltrating tissue was traversed by prominent, thickened bridging perirenal (Kunin) septa, producing the characteristic shaggy, spiculated contour described as the “hairy kidney” appearance. The renal parenchyma itself enhanced normally and no focal renal mass was identified.

The infiltrative process extended medially to involve the renal hila and the proximal ureters, resulting in moderate bilateral hydroureteronephrosis with a smooth, tapering transition at the level of the mid-ureters. Continuous with the perirenal tissue, a circumferential mantle of soft tissue was seen surrounding the abdominal aorta, extending superiorly to the level of the descending thoracic aorta and inferiorly to the common iliac artery origins. This periaortic tissue completely encircled the vessel, including its posterior

aspect, and extended along the origins of the coeliac axis, superior mesenteric artery and both renal arteries without causing significant luminal narrowing. The aorta was not displaced anteriorly from the vertebral column.

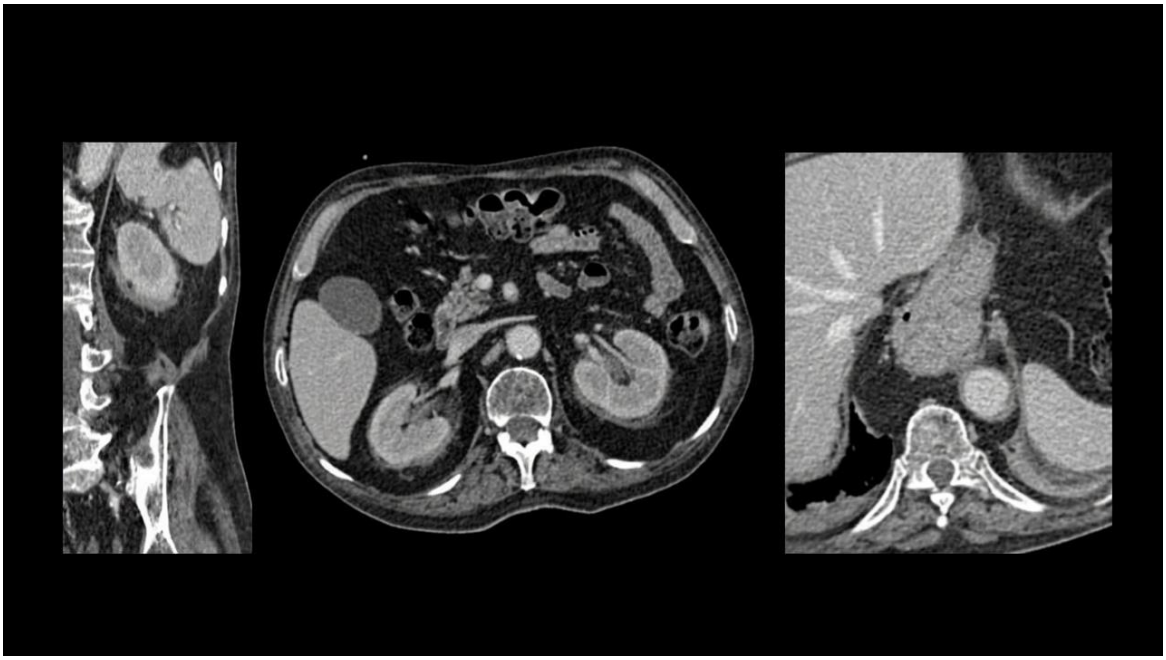

Figure 2: Axial and multiplanar contrast-enhanced CT images of the abdomen demonstrating bilateral symmetric perinephric soft-tissue infiltration with thickened bridging perirenal septa producing the classic "hairy kidney" appearance, together with circumferential periaortic soft tissue ("coated aorta" sign) that completely encircles the vessel without anterior displacement from the vertebral column.

Extension of the study to include the thorax revealed smooth thickening of the interlobular septa in a predominantly peripheral and basal distribution, associated with mild subpleural reticulation and small areas of ground-glass attenuation. Diffuse thickening of the pericardium was noted along with a small pericardial effusion. Within the cardiac silhouette, an infiltrative, mildly enhancing soft-tissue mass was identified in the region of the right atrioventricular groove extending into the right atrial wall, consistent with the reported right atrial pseudotumour of ECD.

Given the clinical history of polyuria and polydipsia, magnetic resonance imaging of the sella and orbits was undertaken. This demonstrated loss of the normal T1 hyperintense posterior pituitary bright spot, together with mild thickening and homogeneous enhancement of the pituitary infundibulum. Within the orbits, bilateral symmetric intraconal soft tissue was identified surrounding the optic nerve sheath complexes.

Whole-body 99mTc-MDP bone scintigraphy demonstrated intense, symmetric, bilateral tracer accumulation in the distal femora, proximal and distal tibiae, with relative sparing of the epiphyses and normal uptake in the axial skeleton — the "hot knees" appearance corresponding to the radiographic osteosclerosis.

The constellation of bilateral symmetric metadiaphyseal osteosclerosis, hairy kidneys, coated aorta, right atrial pseudotumour, infundibular thickening and bilateral orbital infiltration was considered highly characteristic of Erdheim–Chester disease. The principal differential considerations of idiopathic retroperitoneal fibrosis and IgG4-related disease were regarded as unlikely, as neither typically produces symmetric long-bone osteosclerosis, and periaortic tissue in idiopathic retroperitoneal fibrosis characteristically spares the posterior aortic wall while displacing the aorta anteriorly.

A percutaneous image-guided core biopsy of the perinephric soft tissue was performed. Histopathological examination revealed sheets of foamy, lipid-laden histiocytes admixed with scattered lymphocytes, plasma cells and occasional Touton-type giant cells, set within a dense fibrous stroma. Immunohistochemistry demonstrated strong positivity for CD68 and Factor XIIIa, with the histiocytes negative for CD1a, langerin and S100, thereby excluding Langerhans cell histiocytosis and Rosai–Dorfman disease. Molecular testing identified a BRAF V600E mutation, confirming the diagnosis of Erdheim–Chester disease.

The patient was referred for haemato-oncological management and commenced on targeted BRAF inhibitor therapy. Bilateral ureteric stenting was undertaken to relieve the obstructive uropathy, with subsequent improvement in renal function, and desmopressin was initiated for central diabetes insipidus. Follow-up CECT at six months demonstrated a measurable reduction in the thickness of both the perinephric and the periaortic soft tissue with

improvement in the degree of hydronephrosis, and the patient reported substantial relief of his bone pain.

3. Discussion

This case illustrates the characteristic multisystem imaging phenotype of Erdheim–Chester disease and demonstrates how the recognition of a distinctive radiological pattern can shorten what is otherwise a notoriously protracted diagnostic journey. Imaging findings carry greater specificity than histopathology in ECD.

The skeletal manifestations were the most diagnostically decisive feature: bilateral symmetric metadiaphyseal osteosclerosis of the long bones with epiphyseal sparing is the single most characteristic imaging finding and should prompt evaluation for the disease even in the absence of symptoms.

The abdominal findings- hairy kidney and coated aorta- are equally characteristic. The distinction from idiopathic retroperitoneal fibrosis is critical: ECD periaortic tissue completely encircles the aorta (including posteriorly) without displacing it anteriorly, and is accompanied by the symmetric long-bone changes that RPF lacks.

Cardiac (right atrial pseudotumour), orbital and neuroendocrine (loss of posterior pituitary bright spot with infundibular thickening producing central diabetes insipidus) involvement are well-recognised and frequently clinically silent.

Histology shows foamy CD68-positive, CD1a-negative histiocytes but is not specific in isolation; the diagnosis requires integration with the characteristic imaging phenotype. Identification of BRAF V600E mutation enabled targeted therapy, which produced measurable regression of soft-tissue disease at six months. In the era of MAPK-targeted therapy, prompt radiological recognition has direct therapeutic consequence.

4. Conclusion

Erdheim–Chester disease is a rare histiocytic neoplasm whose diagnosis rests substantially upon the recognition of a characteristic imaging phenotype. The combination of bilateral symmetric metadiaphyseal osteosclerosis of the long bones with epiphyseal sparing, symmetric perinephric infiltration producing the hairy kidney appearance, and circumferential periaortic soft tissue constituting the coated aorta sign should be regarded as strongly suggestive of the diagnosis, particularly when accompanied by a right atrial pseudotumour, orbital infiltration or infundibular thickening. Because histopathology in ECD is frequently non-specific, the radiologist bears primary responsibility for raising the possibility of the disease and for directing biopsy to an appropriate site. Familiarity with these findings should be considered essential knowledge for the practising radiologist.

References

[1] Goyal G, et al. Erdheim-Chester disease: consensus recommendations for evaluation, diagnosis, and treatment in the molecular era. Blood. 2020;135(22):1929-1945.
[2] Diamond EL, et al. Consensus guidelines for the diagnosis and clinical management of Erdheim-Chester disease. Blood. 2014;124(4):483-492.
[3] Haroche J, et al. High prevalence of BRAF V600E mutations in Erdheim-Chester disease but not in other non-Langerhans cell histiocytoses. Blood. 2012;120(13):2700-2703.
[4] Dion E, et al. Bone involvement in Erdheim-Chester disease: imaging findings including periostitis and partial epiphyseal involvement. Radiology. 2006;238(2):632-639.
[5] Dion E, et al. Imaging of thoracoabdominal involvement in Erdheim-Chester disease. AJR Am J Roentgenol. 2004;183(5):1253-1260.
[6] Serratrice J, et al. “Coated aorta”: a new sign of Erdheim-Chester disease. J Rheumatol. 2000;27(6):1550-1553.
[7] Haroche J, et al. Cardiac involvement in Erdheim-Chester disease. Circulation. 2009;119(25):e597-e598.
[8] Aswani Y, et al. Imaging in Erdheim-Chester disease. RadioGraphics. 2024;44(11):e240011.